

# Design of Extraction Line Optics for the ILC Interaction Regions with 20 mrad and 2 mrad Crossing Angles

Y. Nosochkov, K. Moffeit, A. Seryi, C. Spencer, M. Woods  
*Stanford Linear Accelerator Center, Menlo Park, CA 94025, USA*

B. Parker  
*Brookhaven National Laboratory, Upton, NY 11973, USA*

D. Angal-Kalinin, R. Appleby  
*ASTeC, Daresbury Laboratory, Warrington, WA4 4AD, England*

The studies of the ILC extraction line design have been carried out by the SLAC-BNL-UK-France task force collaboration. In this paper, we describe two options of the extraction optics for the 20 mrad horizontal crossing angle in the Interaction Region (IR), and one option of the 2 mrad extraction optics. The main functions of the extraction line are to transport the primary beam and beamstrahlung photons to dumps with acceptable beam loss, and to provide the necessary optics for beam diagnostics. The presented 20 mrad and 2 mrad optics are designed for up to 1 TeV and 0.5 TeV Center of Mass (CM) energy, respectively. The upgrade of this 2 mrad design to 1 TeV CM and a separate version of the 2 mrad design are presented in a separate report [1].

## 1. INTRODUCTION

At the International Linear Collider (ILC), the  $e^+e^-$  collisions will create the high power spent beams: the disrupted primary beam and the beamstrahlung photons. Since the total power in these beams will be as large as 11.3 MW at 0.5 TeV Center of Mass (CM) energy and 18.1 MW at 1 TeV CM, they have to be carefully transported to dumps without excessive loss on the extraction magnets. The additional complication is that the collision creates a very long low energy tail in the disrupted beam and increases the beam angular divergence. The extraction designs for 20 mrad and 2 mrad horizontal crossing angle at the Interaction Point (IP) are presented below. The advantage of the 2 mrad crossing angle is that the geometric luminosity reduction is small, hence a crab cavity may not be required on the incoming line. However, the small beam separation after IP leads to a complicated extraction design with shared Final Focus (FF) magnets. The 20 mrad crossing angle allows an independent extraction line, but a crab cavity is needed to avoid the luminosity loss. The extraction optics requires a large chromatic acceptance to minimize the beam loss caused by overfocusing of low energy particles. The additional design requirement is that the optics includes a diagnostic section for post-IP measurements of beam energy and polarization. The presented 20 mrad and 2 mrad optics are designed for up to 1 TeV and 0.5 TeV CM energy, respectively. The upgrade of this 2 mrad option to 1 TeV CM energy and the second version of 2 mrad design are presented in a separate report [1].

## 2. DESIGN OF THE 20 MRAD EXTRACTION LINE

The 20 mrad crossing angle provides a sufficient beam separation for an independent extraction line as shown schematically in Fig. 1. In this design, the primary  $e^+$  or  $e^-$  beam and the beamstrahlung photons share the same beam line and a dump. Based on the superconducting (SC) compact quadrupole design [2], it is possible to have the first FF and extraction quadrupoles at the same distance after IP as shown in Fig. 2. The advantage of the side-by-side positions of these quadrupoles is that the extraction quad can locally compensate the fringe field of the FF quad on the extraction line. At the same time, the first extraction quadrupole is made relatively weak to minimize its fringe field on the incoming line.

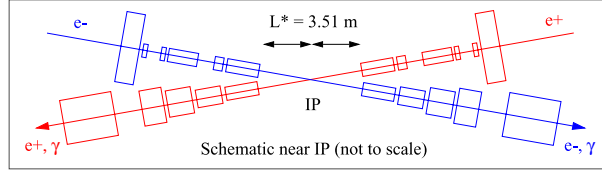


Figure 1: Schematic of the 20 mrad crossing.

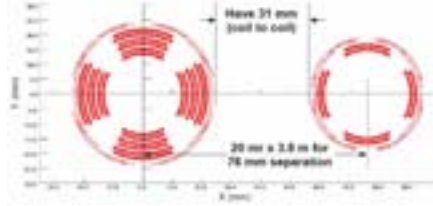


Figure 2: Cross section of the first FF (left) and extraction (right) SC quadrupoles after IP.

## 2.1. Optics

Two options of the 20 mrad extraction optics are compared below. Both designs have identical lattice but the opposite quadrupole polarities. Lattice functions for these options are shown in Fig. 3, where the IP is at  $s=0$  and the dump is at  $\approx 180$  m. The lattice consists of the initial multi-quadrupole system, followed by the two vertical chicanes for beam diagnostics, and the weak quadrupole doublet for low energy focusing at the dump. It is planned that quadrupoles up to  $s = 11.5$  m will be superconducting, followed by the 2 m gap for the incoming crab-cavity, and the warm magnets downstream. The quadrupole parameters for the optics with the first horizontally focusing (F) quadrupole are shown in Table I for 1 TeV CM energy, where  $L$ ,  $B'$ , and  $R$  are the quad length, gradient, and the radius of beam pipe, respectively. The optics with the first defocusing (D) quad has the opposite sign of all

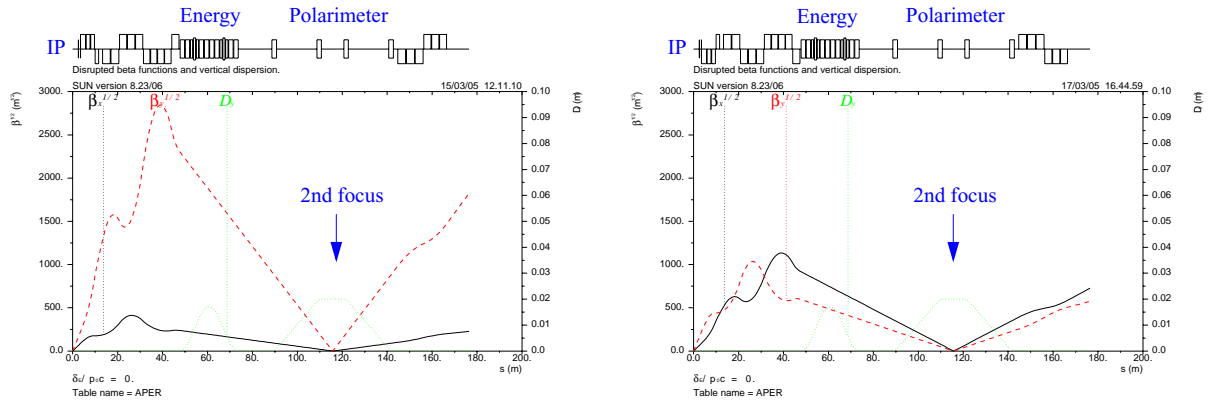


Figure 3: Lattice functions in the 20 mrad extraction line with the first F quad (left) and D quad (right).

Table I: Quadrupole parameters for the 20 mrad extraction line at 1 TeV CM.

| Name      | L [m]  | B' [T/m] | R [mm] | Name         | L [m]  | B' [T/m] | R [mm] |
|-----------|--------|----------|--------|--------------|--------|----------|--------|
| QFEX1A    | 2.2    | 41.667   | 12     | QFEX3C       | 3.2752 | 20.690   | 58     |
| QFEX1B    | 1.7074 | 70.588   | 17     | QDEX4A       | 2.8409 | -16.901  | 71     |
| QFEX1C    | 1.7074 | 50.0     | 24     | QDEX4B,4C,4D | 2.8409 | -15.584  | 77     |
| QDEX2A    | 1.4752 | -40.0    | 30     | QFEX5        | 3.2191 | 16.901   | 71     |
| QDEX2B,2C | 3.4789 | -27.907  | 43     | QDEX6A,6B,6C | 3.5631 | -3.2     | 250    |
| QFEX3A    | 3.2752 | 27.907   | 43     | QFEX7A,7B,7C | 3.1872 | 3.2      | 250    |
| QFEX3B    | 3.2752 | 26.087   | 46     |              |        |          |        |

Both F and D lattice options have identical diagnostic sections which include the two vertical chicanes for energy and polarization measurements, where the maximum vertical dispersion is 1.7 and 2 cm, respectively. The optics provides the 2nd focal point at center of the polarimeter chicane to attain the required  $<100\mu\text{m}$  beam size. The energy spectrometer will measure the average beam energy by producing synchrotron radiation (SR) in wiggler magnets along the  $\pm 2$  mrad beam directions in the energy chicane [4]. The polarization measurement will be performed by a Compton polarimeter, with the Compton IP [5] located at the 2nd focus. This measurement requires that the value of  $R_{22}$  matrix term between the IP and the Compton IP is close to -0.5 or +0.5. The +0.5 value is more optimal, but it requires an additional  $180^\circ$  focusing section which would reduce the chromatic acceptance. In the present F and D optics the  $R_{22}$  value is -0.14 and -0.53, respectively. This shows that the D optics is better for the polarization diagnostics. The first D quadrupole also improves the focusing of the low energy secondary particles vertically deflected in the detector solenoid. [6].

## 2.2. Particle Tracking

In tracking simulations, the disrupted beam was transported from IP to dump using the DIMAD code [7]. Two cases were considered: 1) ideal collisions at IP, and 2) collisions with large vertical beam-to-beam offset  $\Delta y$  which maximizes the disrupted beam vertical divergence. Table II compares the maximum electron and photon angles at IP and the lowest relative energy  $E_{min}/E_0$  in the beam for the proposed nominal and high luminosity parameters at 0.5 TeV and 1 TeV CM energies [3]. The disrupted energy distribution is shown in Fig. 4.

One can see that at ideal IP collisions the disrupted beam size is larger in the horizontal plane, but the vertical size can dominate at a large  $\Delta y$ . The low energy tail increases with beam energy and it is maximized in the high luminosity options. Summary of the total beam power loss is presented in Table III. At  $\Delta y \neq 0$  (from Table II), the beam loss is enhanced by the large IP vertical angles. The tracking showed that most of the loss occurs in the low energy tail for the relative energies of  $E/E_0 < 40\%$ . Because of the initial horizontal focusing, the optics with the first F quad provides a lower beam loss at ideal beam collisions. But the D optics has a lower loss when  $\Delta y$  is large.

The study of tolerable power loss on extraction magnets is not fully complete at this time. But based on the

Table II: Maximum angle and the lowest energy in the disrupted electron and photon beams at IP.

| $E_{CM}$ [TeV]<br>luminosity<br>option | Ideal Collision at IP |  |  | Large Vertical Offset $\Delta y$ at IP |                      |  |  |
|--|-----------------------|--|--|--|----------------------|--|--|
|  | $E_{min}/E_0$<br>[%]  | Electron<br>$X'_{max}/Y'_{max}$<br>[ $\mu\text{rad}$ ] | Photon<br>$X'_{max}/Y'_{max}$<br>[ $\mu\text{rad}$ ] | $\Delta y$<br>[nm]                     | $E_{min}/E_0$<br>[%] | Electron<br>$X'_{max}/Y'_{max}$<br>[ $\mu\text{rad}$ ] | Photon<br>$X'_{max}/Y'_{max}$<br>[ $\mu\text{rad}$ ] |
| 0.5 nominal                            | 36                    | 529 / 253  | 369 / 212  | 200                                    | 36                   | 474 / 674  | 366 / 537  |
| 0.5 high                               | 17                    | 1271 / 431   | 723 / 320  | 120                                    | 17                   | 1280 / 1415  | 782 / 1232   |
| 1.0 nominal                            | 20                    | 496 / 159  | 271 / 148  | 100                                    | 19                   | 423 / 566  | 279 / 408  |
| 1.0 high                               | 6.3                   | 2014 / 489   | 937 / 296  | 80                                     | 6.2                  | 1731 / 1592  | 974 / 1200   |

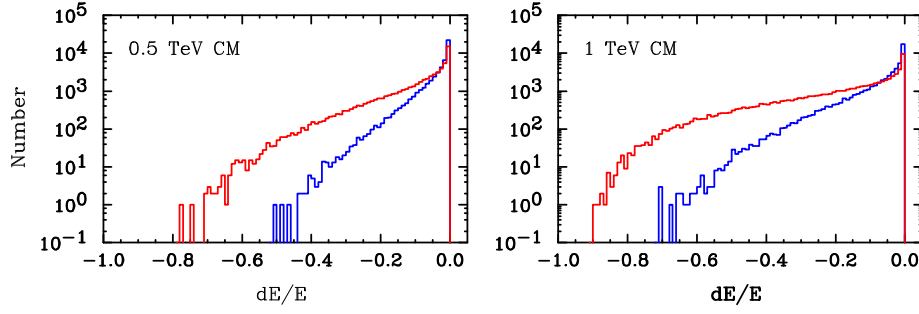


Figure 4: Disrupted energy distribution  $\Delta E/E_0$  for 0.5 and 1 TeV CM energy for  $7 \times 10^4$  particles. Each plot shows the nominal and high luminosity options, where the latter has a longer tail.

Table III: Total beam power loss in the 20 mrad extraction line.

| Luminosity Option  |                   | Nominal |        |      |      | High |     |     |     |
|--------------------|-------------------|---------|--------|------|------|------|-----|-----|-----|
| $E_{CM}$ [TeV]     |                   | 0.5     |        | 1.0  |      | 0.5  |     | 1.0 |     |
| Optics Option      |                   | F       | D      | F    | D    | F    | D   | F   | D   |
| Total loss<br>[kW] | $\Delta y = 0$    | 0       | 0.0003 | 0.12 | 0.46 | 1.8  | 3.5 | 48  | 49  |
|                    | $\Delta y \neq 0$ | 0.006   | 0.001  | 3.9  | 2.0  | 14   | 10  | 325 | 274 |

current calculations of beam loss distribution in the magnets, it appears that the power loss is acceptable in the 0.5 TeV and 1 TeV CM nominal luminosity options. In these cases no loss occurred on the sensitive SC quads, and the losses in other magnets are reasonably small. In the 0.5 TeV CM high luminosity option, the beam loss may be acceptable in the D optics where the loss on SC quads is  $\sim 2$  W/m. In the corresponding F optics, the SC losses are too high ( $\sim 50$  W/m) in the case with a large  $\Delta y$  offset. And the losses are not acceptable in the 1 TeV CM high luminosity option, but there is a plan to modify this parameter set in order to reduce the low energy tail.

Based on the comparison of the F and D optics, we select the D option as more optimal since it provides the better conditions for the polarization diagnostics, has a lower secondary particle loss in the SC quads and a comparable loss for the primary beam. More optimization will be performed on this optics.

### 3. DESIGN OF THE 2 MRAD EXTRACTION LINE

The main complication of the 2 mrad extraction line is that the small beam separation after IP requires that the spent beam goes off-center and at an angle through the aperture of the FF quadrupoles and sextupoles, while the incoming beam is on center in these magnets. The consequence is that the FF magnets require rather large apertures to accommodate the two electron beams and the beamstrahlung photons. We assume that the photons have  $\pm 0.5$  mrad maximum angles at IP which is consistent with the nominal luminosity options. In this scheme, the shared FF magnets can not be solely optimized for the extracted beam since they are constrained by the incoming optics. The beam offset in the FF magnets creates a non-linear horizontal dispersion in the extracted beam. Therefore, the use of downstream bending magnets is required to control the dispersion and to provide a sufficient separation with the incoming line. Finally, the electron and photon beams diverge into separate beam lines and require separate dumps. The schematic of the 2 mrad crossing near IP is shown in Fig. 5, where the shared FF magnets are the QD0, QF1 quadrupoles and SD0, SF1 sextupoles. The first independent extraction quadrupole is QEXF1.

In this scheme, the QD0, SD0 and SF1 are the large bore SC magnets with aperture radius of 45 mm, 95 mm and 130 mm, respectively. The QF1 is a warm iron quadrupole with 10 mm aperture for the incoming beam. The extracted beam passes horizontally outside of the QF1 aperture through its coil pocket between the quad poles. The non-linear field in the QF1 pocket was pre-calculated [8] and modeled as a multipole field on the extraction line. The

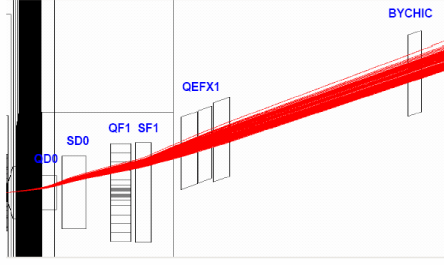


Figure 5: Schematic of the 2 mrad crossing. The extracted beam goes out of IP (at left) at an offset and angle in the shared FF magnets. The incoming beam comes to IP along the horizontal axis.

first extraction quadrupole QEXF1 is at about 26 m after the IP. The complication is that it has a large aperture of 83 mm for the spent electrons and photons and is separated horizontally only by 109 mm from the incoming beam. The small separation and the requirement that the QEXF1 fringe field on the incoming line is small makes it difficult to design such a magnet. Nevertheless, two designs have been suggested. The first one is the SC super septum quadrupole design [9] which allows a large aperture for the extracted beams and a hole in the iron for the incoming beam where the field is suppressed to a few gauss. The second proposal is to use a Panofsky style water cooled septum magnet [8] which may also provide large extraction aperture for a small beam separation. Both of these magnet designs need further investigation.

The 2 mrad extraction beta functions and linear dispersion for 0.5 TeV CM nominal option are shown in Fig. 6. The initial shared FF magnets are optimized for both the incoming and extracted beams. Due to the extracted beam offset and bending in the FF magnets, it is more difficult to contain the low energy orbits in the 2 mrad optics than in the 20 mrad design. To minimize the low energy losses, a dedicated vertical chicane is included for collimation of the low energy tail. To further increase the chromatic acceptance, two sextupoles are included in the optics. At present, the 2 mrad lattice does not include the diagnostic chicanes. These will be added in the near future. But the 2nd focal point with the same as at IP 2 mrad horizontal orbit angle, as required for polarimetry, is included.

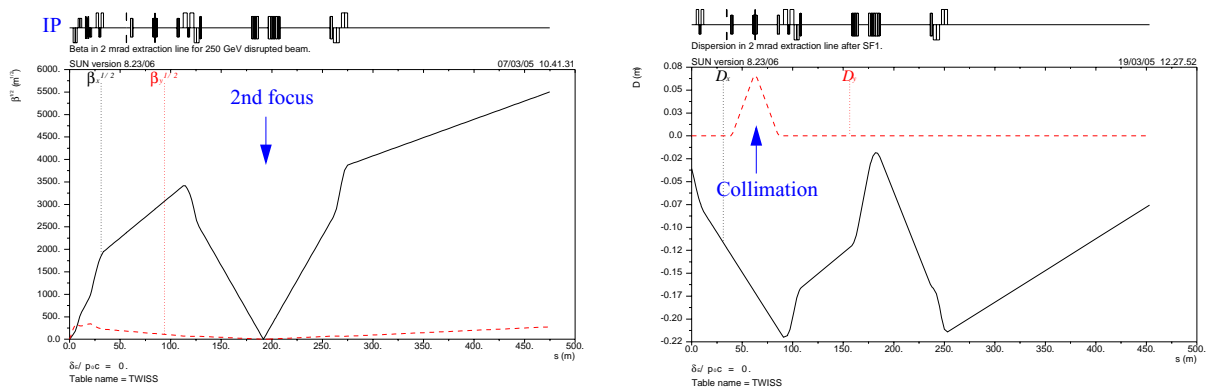


Figure 6: Beta functions (left) and dispersion (right) in the 2 mrad extraction line.

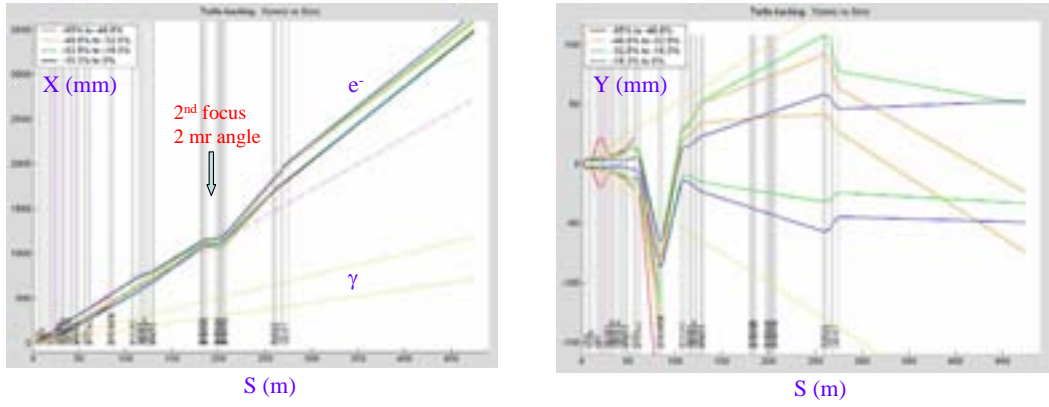


Figure 7: Horizontal (left) and vertical (right) envelopes of the extracted beam for  $\Delta E/E_0$  from 0 to -65% for 0.5 TeV CM nominal luminosity option.

place. The tracking showed that the beam loss is acceptable in the 0.5 and 1 TeV CM nominal luminosity options, and there was no loss on the SC magnets. It was estimated that the vertical chicane collimator intercepts 23 kW of the low energy tail in the 0.5 TeV CM nominal case. However, in the high luminosity options, the beam loss on the SC magnets is unacceptably high. Further optimization is needed to reduce the loss in these cases.

## 4. CONCLUSION

We presented the preliminary optics designs for the 20 mrad and 2 mrad ILC extraction lines. Both optics provide a sufficient acceptance for a tolerable beam loss in the ILC nominal luminosity options. Further optimization is needed to reduce the beam loss in the high luminosity options. The 20 mrad design includes the required optics for beam diagnostics. The 2 mrad optics will be further developed to add the diagnostic chicanes. The future studies will also include a detailed magnet design, optimization of beam spot at the dump and collimation options.

## Acknowledgments

We thank T. Maruyama and M. Woodley for providing the fine graphics of the GEANT tracking and the ILC layout. This work is supported by Department of Energy contract DE-AC02-76SF00515.

## References

- [1] R. Appleby, *et al.*, "The 2 mrad Horizontal Crossing Angle IR Layout for a TeV ILC," these proceedings.
- [2] B. Parker, *et al.*, "Compact Superconducting Final Focus Magnet Options for the ILC," to be published in Proceedings of the 2005 Part. Acc. Conf., Knoxville, TN, USA (2005).
- [3] T. Raubenheimer, <http://www-project.slac.stanford.edu/ilc/acceldev/beamparameters.html> (Feb. 28, 2005).
- [4] D. Cinabro, *et al.*, IPBI TN-2003-1 (2003).
- [5] K.C. Moffeit, M. Woods, IPBI TN-2003-2 (2003).
- [6] T. Maruyama, unpublished.
- [7] <http://www.slac.stanford.edu/accel/ilc/codes/dimad/>.
- [8] C. Spencer, unpublished.
- [9] B. Parker, unpublished.
- [10] D.C. Carey, K.L. Brown, Ch. Iselin, "Decay TURTLE," SLAC-246 (1982).